JACS
JOURNAL OF THE AMERICAN CHEMICAL SOCIETY
Article
pubs.acs.org/JACS

Solid-State Reversible Nucleophilic Addition in a Highly Flexible MOF

Arianna Lanza,*[,†,‡] Luzia S. Germann,[†,§] Martin Fisch,[†,‡] Nicola Casati,[‡] and Piero Macchi*[,†]

[†]Department of Chemistry and Biochemistry, University of Bern, Freiestrasse 3, 3012 Bern, Switzerland
[‡]Swiss Light Source, Paul Scherrer Institute, CH-5232 Villigen, Switzerland

Supporting Information

ABSTRACT: A flexible and porous metal−organic framework, based on Co^{II} connectors and benzotriazolide-5-carboxylato linkers, is shown to selectively react with guest molecules trapped in the channels during the sample preparation or after an exchange process. Stimulated by a small crystal shrinking, upon compression or cooling, the system undergoes a reversible, nonoxidative nucleophilic addition of the guest molecules to the metal ion. With dimethylformamide, only part of the penta-coordinated Co atoms transform into hexa-coordinated, whereas with the smaller methanol all of them stepwise increase their coordination, preserving the crystallinity of the solid at all stages. This extraordinary example of chemisorption has enormous implications for catalysis, storage, or selective sieving.

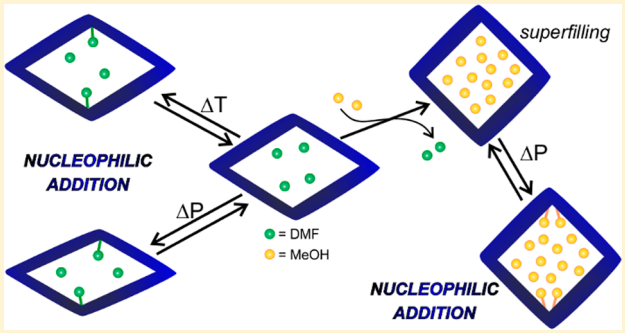

INTRODUCTION

The growing interest in the synthesis and properties of porous metal−organic frameworks (MOFs) stems from their potential applications for heterogeneous catalysis, sensing, separation, and storage of small molecules.[1−4] MOFs combine the potentially unlimited tailorability typical of organic materials with the properties of porous inorganic frameworks.

MOFs that feature stereochemically accessible unsaturated metal centers are promising catalysts or (selective) absorbents. However, the unsaturation of one or more metal centers is not a sufficient condition, because the framework itself must be capable of including or expelling reactant molecules. This implies that the MOF must have sufficient void space for the migration of guest molecules inside the channels and/or that the framework can flexibly rearrange upon the insertion of the guest in the metal coordination sphere.

In the literature, a wide variety of so-called "breathing" MOFs has been reported.[5] Some of them show remarkable expansion or contraction of the framework upon sorption or desorption of guest molecules. This breathing can be autonomous, if the MOF immediately reacts upon exposure to sufficient quantity of the guests (in liquid or vapor state), or stimulated, if the guest molecules are pumped into the MOF's channels. The latter can be obtained, for example, through the application of pressure.

High-pressure (HP) techniques are quite common for studying the dynamic behavior of minerals or technologically relevant inorganic materials. However, only a handful of studies is available on MOFs or hybrid materials mechanically compressed above 1 GPa.[6−15] These studies have provided relevant observations: (i) porous metal−organic materials are, as expected, softer than purely inorganic porous materials (e.g., zeolites), but they can feature a larger hardness compared to organic molecular crystals, although having in general much lower density.[16] (ii) MOFs frequently undergo reversible or irreversible amorphization transformations within few GPa. (iii) The compressibility and stability of porous frameworks strongly depend on the presence of guests in the pores; in fact, empty frameworks are more compressible and fragile compared to guest-containing ones. (iv) Pressure may induce significant uptake of additional guest molecules. (v) MOFs may exchange the guest molecules, if the pressure transmitting medium (PTM) used to apply the external force contains molecules that are able to penetrate the pores and bind to the framework.

By varying metal centers, oxidation states, organic linkers, guest molecules, stereochemical features, etc., the potential and complexity of MOFs can be tuned according to the desired properties. Efforts to rationalize the synthesis of frameworks with specific features would therefore benefit from comparative studies involving systematic variations of their structure. In this context, we started a project aimed at investigating the role of controlled structural modifications on the physicochemical properties of a family of isostructural MOFs. During this study, we observed in $[Co_3(OH)_2btca_2]$ (hereinafter, **Co-btca**, where btca = benzotriazolide-5-carboxylato) an unusual solid-state chemical reaction, which consists of a nonoxidative nucleophilic addition at the metal node, favored by temperature- or pressure-induced crystal shrinking. Some metal−organic complexes have been reported to undergo P-induced non-oxidative nucleophilic addition, leading to an increase of the coordination number and in some cases to the polymerization of complexes into 1D chains.[17−19] Some other relevant modifications on the metal nodes have been reported, mainly

Received: July 31, 2015
Published: September 24, 2015

DOI: 10.1021/jacs.5b09231
J. Am. Chem. Soc. 2015, 137, 13072−13078

Table 1. Crystal Data and Refinement for Most Significant Phases of Co-btca

T/K	RT	198(2)	RT	RT
P/GPa	ambient	ambient	0.4(2)	ambient (in DAC)
guest molecules	DMF	DMF	DMF	MeOH
compound formula	$[Co_3(OH)_2btca_2]\cdot 2$ DMF	$[Co_3(OH)_2btca_2(DMF)]\cdot$DMF	$[Co_3(OH)_2btca_2(DMF)]\cdot$DMF$\cdot H_2O$	$[Co_3(OH)_2btca_2]\cdot 2$ MeOH[a]
sum formula, M_r/g mol^{-1}		$Co_3C_{20}H_{22}N_8O_8$, 679.24	$Co_3C_{20}H_{24}N_8O_9$, 697.26	$Co_3C_{16}H_{16}N_6O_8$, 597.14[a]
crystal system	monoclinic	triclinic	triclinic	monoclinic
space group, Z	$C2/c$, 4	$P-1$, 2	$P-1$, 2	$C2/c$, 4
unit cell dimensions:				
a/Å	17.7835(6)	10.9204(7)	10.852(3)	17.6286 (10)
b/Å	12.7818(4)	10.9603(7)	10.9126(6)	13.0929(12)
c/Å	11.2254(3)	11.0587(5)	11.1478(6)	11.0727(6)
α/°	90	83.328(4)	84.499(5)	90
β/°	95.180(3)	87.023(4)	88.211(9)	95.599(5)
γ/°	90	70.330(6)	66.360(12)	90
V/Å^3	2541.17(14)	1237.83(13)	1203.8(3)	2543.5(3)
primitive V/Å^3	1270.59			1271.75
molar V/cm^3 mol^{-1}	382.57	372.71	362.2	382.92
θ range/°	1.965—28.164	1.854—28.088	1.835—28.673	1.941—28.586
reflections (unique), R_{int}	8742 (2846), 0.0519	10701 (5426), 0.0443	7162 (1431), 0.0683	7679 (1440), 0.0523
parameters (restraints)	177 (24)	358 (24)	194 (111)	143 (3)
goodness-of-fit on F^2	1.032	1.116	1.115	1.039
R indices $[I > 2\sigma(I)]$	$R_1 = 0.0486$, $wR_2 = 0.1052$	$R_1 = 0.0580$, $wR_2 = 0.1236$	$R_1 = 0.0743$, $wR_2 = 0.1726$	$R_1 = 0.0600$, $wR_2 = 0.1506$
largest diff. peak and hole	0.931 and −0.934 e Å^{-3}	0.951 and −0.589 e Å^{-3}	0.850 and −0.901 e Å^{-3}	0.707 and −0.811 e Å^{-3}

T/K	RT	RT	RT	RT
P/GPa	0.3(2)	0.9(2)	2.2(2)	ambient (in DAC, after decompression)
guest molecules	MeOH	MeOH	MeOH	MeOH
compound formula[a]	$[Co_3(OH)_2btca_2(MeOH)]$	$[Co_9(OH)_6btca_6(MeOH)_2]$	$[Co_3(OH)_2btca_2(MeOH)_2]$	$[Co_3(OH)_2btca_2]$
sum formula,[a] M_r/g mol^{-1}	$Co_3C_{15}H_{12}N_6O_7$, 565.10	$Co_9C_{44}H_{32}N_{18}O_{20}$, 1663.25	$Co_3C_{16}H_{16}N_6O_8$, 597.14	$Co_3C_{14}H_8N_6O_6$, 533.05
crystal system	triclinic	monoclinic	monoclinic	monoclinic
space group, Z	$P-1$, 2	$C2/c$, 4	$C2/c$, 4	$C2/c$, 4
unit cell dimensions:				
a/Å	11.0437(17)	16.8014(10)	16.894(3)	18.418(3)
b/Å	11.0107(5)	14.1730(10)	14.014(3)	11.576(4)
c/Å	11.0222(5)	33.1813(18)	11.0033(14)	11.0520(15)
α/°	83.364(4)	90	90	90
β/°	85.871(8)	96.641(4)	98.287(12)	94.124(13)
γ/°	77.346(8)	90	90	90
V/Å^3	1297.5(2)	7848.3(8)	2577.8(7)	2350.3(10)
primitive V /Å^3		3294.19	1288.9	1175.15
molar V/cm^3 mol^{-1}	390.68	393.85	388.09	353.84
θ range/°	1.906—28.770	1.885—23.815	1.896—23.256	2.079—28.778
reflections (unique), R_{int}	7403 (1506), 0.0701	21073 (3502), 0.0858	6464 (1111), 0.0758	6902 (1262), 0.0951
parameters (restraints)	150 (61)	218 (7)	81 (43)	70 (1)
goodness-of-fit on F^2	1.051	1.040	1.317	1.141
R indices $[I > 2\sigma(I)]$	$R_1 = 0.0557$, $wR_2 = 0.1368$	$R_1 = 0.0709$, $wR_2 = 0.1769$	$R_1 = 0.1111$, $wR_2 = 0.3105$	$R_1 = 0.0920$, $wR_2 = 0.2341$
largest diff. peak and hole	0.389 and −0.508 e Å^{-3}	0.705 and −0.462 e Å^{-3}	1.004 and −1.003 e Å^{-3}	0.985 and −1.280 e Å^{-3}

[a]The SQUEEZE procedure was used, therefore, the reported formulas and all derived values are underestimated as they do not take the squeezed guests into account.

induced by high temperature or solvent mediated.[20−24] However, the T- or P- stimulated reactivity of MOF nodes with extra framework molecules has never been reported so far, therefore we investigated in detail the roles played by temperature, pressure, and guest molecules, and we report here the most relevant observations for **Co-btca**.

RESULTS

At ambient conditions, the crystal structure of **Co-btca** (space group $C2/c$) contains two independent Co atoms per asymmetric unit: Co1, which sits on a two-fold axis and is octahedrally coordinated, and Co2, which lies on a general position and features a distorted trigonal bipyramidal coordination ($\tau = 0.64$).[25] Because of the site multiplicity, 2/3 of the Co^{II} ions in the crystal are coordinatively unsaturated and potentially ready for a nonoxidative nucleophilic addition by extra-framework molecules. A water-containing form of **Co-btca** was first reported in 2007[26] and classified as a rigid, second-generation porous MOF.[27] Using a different synthetic procedure, we obtained crystalline **Co-btca** containing two

DOI: 10.1021/jacs.5b09231
J. Am. Chem. Soc. 2015, 137, 13072−13078

dimethylformamide (DMF) guest molecules per $[Co_3(OH)_2btca_2]$ formula unit. DMF induces a bigger unit cell, as measured by single crystal X-ray diffraction (SC-XRD): the unit cell volume of the DMF containing **Co-btca** is 2541.17(14) Å^3 compared to the previously reported[26] 2421(3) Å^3 (see Table 1). Nevertheless, the symmetry and the overall framework topology are unchanged. The DMF molecules are disordered over two orientations, and they are trapped in the channels through hydrogen-bonding interactions with the μ_3-OH groups of the framework. With two DMFs per formula unit, the channel voids are not fully occupied, and smaller H_2O guests can also be absorbed from the reaction mixture into the remaining small cavities, during the crystallization process. This hypothesis is supported by thermogravimetric data (see Supporting Information (SI)) that show a weight loss below 373 K, due to water molecules, and further weight losses at higher temperature, due to DMF. We observed a certain variability of the unit cell volume for different samples, though without changes of the crystal structure or the DMF content. This indicates that the amount of water in the channels is also variable, but SC-XRD at ambient conditions cannot unambiguously locate them, suggesting strong dynamic disorder. On the other hand, water molecules could be located by some of the SC-XRD at HP (*vide infra*), where the space confinement reduces the atomic motion.

Low-Temperature Study of Co-btca. On cooling the as-prepared **Co-btca**·2 DMF below 200 K, the small thermal contraction of the framework promoted the additional coordination of one DMF to one Co2, per formula unit (Figure 1 and SI), as observed by accurate multitemperature SC-XRD experiments.

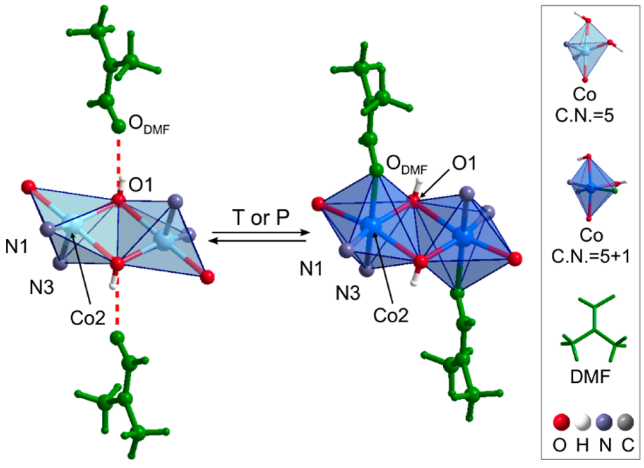

Figure 1. Reversible coordination reaction of the initially H-bonded DMF to a Co center. DMF is colored in green, whereas Co2 is represented with its coordination polyhedra (light blue when pentacoordinated; dark blue when hexacoordinated). The H-bond is a dashed red line. Only one orientation of the disordered H-bonded DMF is shown for clarity.

The extra coordination is evident by the significantly shorter Co···O$_{DMF}$ distance (from 3.440(9) Å at RT vs 2.275(3) Å at 198 K), and it results in a large rearrangement of the Co stereochemistry. In the equatorial plane, the coordination angles at Co2 drastically change: N1—Co2—N3 goes from 124° to 109°, N3—Co2—O1 from 93° to 85°, and O1—Co2—N1 from 140° to 156° (see Figure 1 and Table 2). The low-temperature (LT) phase has space group *P*-1, but the lattice remains very similar to the primitive cell of the high temperature *C*2/*c* phase, with only minor distortions due to the asymmetrization of Co centers. Indeed, the addition reaction involves only one-half of the unsaturated Co atoms and the available DMF molecules, thus in the LT structure there is still one penta-coordinated Co (τ = 0.65) and one noncoordinated DMF per formula unit. No additional reaction was observed upon further cooling down to 100 K. All single crystals we measured were found to split into two twin domains, as a consequence of the symmetry reduction below 200 K. The reaction is fully reversible, with a temperature hysteresis of ∼20 K, in agreement with the DSC analysis, which clearly revealed an endothermic peak (4 kJ mol^{-1}) with onset at 214 K upon heating (see Figure S2 in SI).

HP Study of Co-btca in Nonpenetrating PTM. A very similar reaction occurred when a single crystal of **Co-btca**·2 DMF was compressed in a diamond-anvil cell (DAC) using Daphne oil (DO) as hydrostatic, nonpenetrating PTM. Already at 0.4 GPa, we could observe a *P*-1 phase, similar to the LT one (Table 1 and Figure 2). However, the measured Co−O$_{DMF}$ distance is longer, 2.383(18) Å, and the orientation of the newly coordinated DMF with respect to the metal node is different (see Figure S7 in SI).

Further compression up to 3.6 GPa caused significant contraction of the volume (−17%), especially along the *a* direction, accompanied by a distortion of the binding angles of the carboxylate groups to the Co backbone (see Figure 2 and SI).

As the compression significantly reduced the pore size, the remaining OH···DMF H-bonds broke, and the released DMF molecules reoriented parallel to the pore walls, in order to minimize the sterical hindrance, assuming two disordered orientations. As for the samples investigated at LT, no H_2O molecule was visible, because, if present, they would be disordered over many sites in the channels and too mobile. However, the DMF reorientation occurring at higher pressure makes some H-bond sites available for H_2O molecules to bind. Therefore, we could refine the water position and estimate the content of one molecule per unit formula.

In all our experiments, we could eventually recover the monoclinic ambient pressure phase upon decompression. The DMF guests restored their H-bonding interactions with the framework as well as the positional disorder. Again, the H_2O molecules could not be located by difference Fourier maps, but it is sensible to assume that they were retained, judging from the rather large unit cell volume (2556.6(6) Å^3, see Table S5 in SI).

HP Study of Co-btca in Penetrating PTM. When the HP experiment on **Co-btca**·2 DMF·*y* H_2O was repeated using MeOH:EtOH 4:1 (ME) as PTM, a complete guest exchange occurred instantly after loading the DAC, before any measurable increase of pressure. SC-XRD indicated that MeOH molecules entirely replaced the DMF, forming **Co-btca**·*x* MeOH·*y*′ H_2O. Once again, the water content of the samples is not easy to determine and most likely variable. Hereafter, it will be neglected from the formulas. Anyway, the amount of water does not seem to play a relevant role in the HP behavior of **Co-btca**. No EtOH was found, meaning that the molecule uptake from the PTM was selective under these experimental conditions.

At room pressure, the framework of **Co-btca**·*x* MeOH is isostructural with the DMF-containing analogue, (Figure 3). Part of the guest molecules could be located in the proximity of

DOI: 10.1021/jacs.5b09231
J. Am. Chem. Soc. 2015, 137, 13072−13078

Table 2. Relevant Geometric Parameters for Co-btca as a Function of Temperature

	RT	213 K	208 K	203 K	198 K	173 K
Co2···O_{DMF} /Å	3.440(9)	3.472(8)	3.464(7)	3.465(7)	2.275(3)	2.271(3)
Co2···O_{DMF}′/Å	3.647(8)	3.628(7)	3.628(7)	3.624(7)	3.795(4)	3.787(4)
O1−Co2−N1/°	140.38(13)	140.44(12)	140.48(11)	140.49(11)	156.10(15)	156.14(17)
N1−Co2−N3/°	123.69(14)	123.50(14)	123.27(12)	123.21 (12)	108.87(16)	109.07(18)
N3−Co2−O1/°	93.49(12)	93.44(12)	93.59(10)	93.67(11)	85.40(15)	85.09(16)
τ for Co2	0.64	0.64	0.64	0.64	(0.20)[a]	(0.20)[a]
τ for Co3	0.64	0.64	0.64	0.64	0.65	0.65

[a]In this case Co2 is hexacoordinated, therefore, strictly speaking, a τ value cannot be calculated. This value has been calculated for comparison using the same angles which were previously used to calculate τ for the pentacoordinated form.

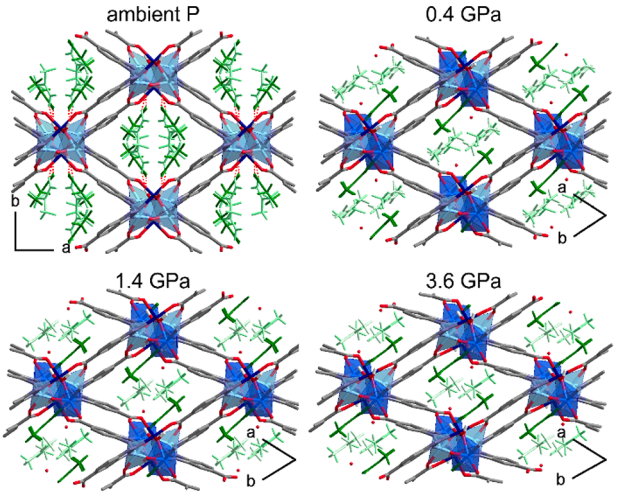

Figure 2. Packing of **Co-btca**·2 DMF·H_2O as a function of P in a nonpenetrating PTM, viewed down the crystallographic *c* axis. Cobalt atoms are represented as in Figure 1. At HP, coordinated and disordered noncoordinated DMF guests are colored in dark and light green, respectively. Water molecules become visible above 0.4 GPa. Framework and water H atoms are omitted for clarity.

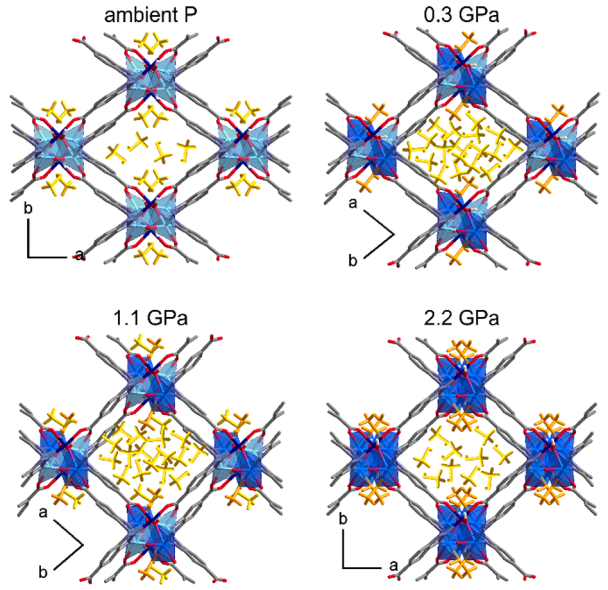

Figure 3. Evolution of the packing of **Co-btca**·*x* MeOH as a function of P using ME as PTM, viewed down the crystallographic *c* axis. Framework H atoms are omitted for clarity. Cobalt atoms are represented as in Figure 1. The guest molecules could be only partially located: coordinated and noncoordinated MeOH guests are colored in dark and light orange, respectively. The estimated amount of disordered MeOH molecules is represented in the channel in random orientations.

unsaturated Co atoms and are possibly frozen in their position by hydrogen bonds with the OH groups of the framework. Nevertheless, they show severe dynamic disorder. Because MeOH is smaller than DMF, some additional molecules are very likely present inside the channels, although dynamically disordered. All data sets were therefore treated with the SQUEEZE procedure implemented in PLATON.[28]

An initial pressure increase to 0.3 GPa was sufficient to promote the coordination of one MeOH to one of the two unsaturated Co centers, similarly to what was observed for DMF. At this pressure, the Co−O_{MeOH} distance, obtained by SC-XRD structure determination, is 2.304(10) Å. In keeping with what observed for **Co-btca**·2 DMF, the increased coordination of Co2 reduces the space group symmetry to *P*−1, with formation of two slightly misaligned twin domains. Further compression to 1.1 GPa showed a contraction of the Co−O_{MeOH} coordination distance (2.256(8) Å). At 2.2 GPa a second addition was observed, and the two newly formed coordination bonds have equal distances (2.354(17) Å). This resulted in a symmetry increase, back to *C*2/*c* and a fully saturated $[Co_3(OH)_2btca_2(MeOH)_2]\cdot x'$ MeOH.

In a second HP-SCXRD experiment, using the same PTM, we found another intermediate phase between 0.6 and 0.9 GPa, where the first nucleophilic addition reaction affected only one-third of the unsaturated Co. This phase is monoclinic *C*2/*c* with a triple *c* axis, compared to the one at ambient conditions (see SI). Upon compression above 1 GPa, a triclinic unit cell was again found, and the diffraction patterns showed 4-fold splitting of the peaks. This feature can be explained with the formation of two pairs of twin domains due to the sequential symmetry breaking that characterizes the phase transitions: monoclinic → triclinic → monoclinic triple cell → triclinic.

Independently from the number of Co atoms that expanded their coordination, the unit cell volume was always found to smoothly increase during the compression, up to a maximum expansion of +3% at 0.9 GPa. This indicates a pressure-induced (super)filling of the framework channels with the PTM. Thereafter, the volume decreased smoothly, yet at 2.2 GPa it was still 1% bigger than at room pressure.

After decompression, in all cases, the recovered crystal was a partially desolvated **Co-btca** with an unprecedented narrow-pore framework, restoring the *C*2/*c* space group, but with a smaller volume (2273.9(12)—2350.3(10) $Å^3$, see Table S7 in SI). Such a significant contraction (ca. −7% with respect to a filled **Co-btca** at ambient P) is caused by the loss of guest MeOH due to evaporation after DAC opening. In fact, MeOH is not stable inside the MOF when left in air (*vide infra*). On

DOI: 10.1021/jacs.5b09231
J. Am. Chem. Soc. 2015, 137, 13072−13078

the other hand, all XRD measures performed on single crystals and powders during the decompression, but before reaching ambient pressure and opening the DAC, confirmed that the guest uptake is fully reversible(see Figure 4).

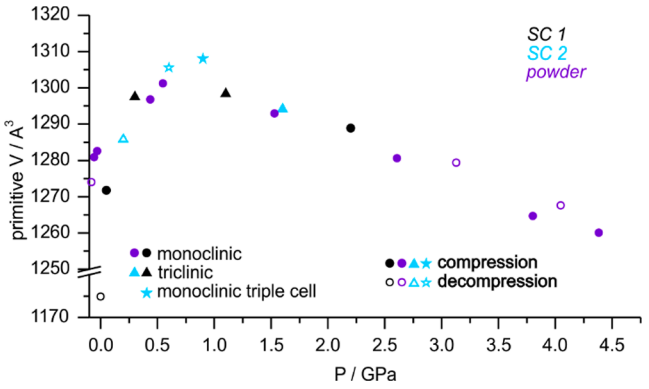

Figure 4. Unit formula volume of **Co-btca**·*x* MeOH as a function of P with ME as penetrating PTM as obtained from powder and SC-XRD. Full and empty symbols indicate measurements obtained during compression and decompression, respectively, while different shapes of the markers indicate the different symmetry of the phases. Different colors distinguish different samples used for the experiments.

Solvent Exchange Experiments. The evidence of guest exchange in a MeOH/EtOH mixture prompted us to test the behavior of **Co-btca**·2 DMF powders immersed in pure liquids, at ambient conditions. Powder X-ray diffraction (P-XRD) experiments, carried out in closed capillaries, evidenced the easy and selective uptake of MeOH from the pure liquid or from ME, as observed by comparing the powder patterns as well as the respective lattice parameters obtained by LeBail fits (see Figure 5 and SI). When a powder was treated with pure EtOH,

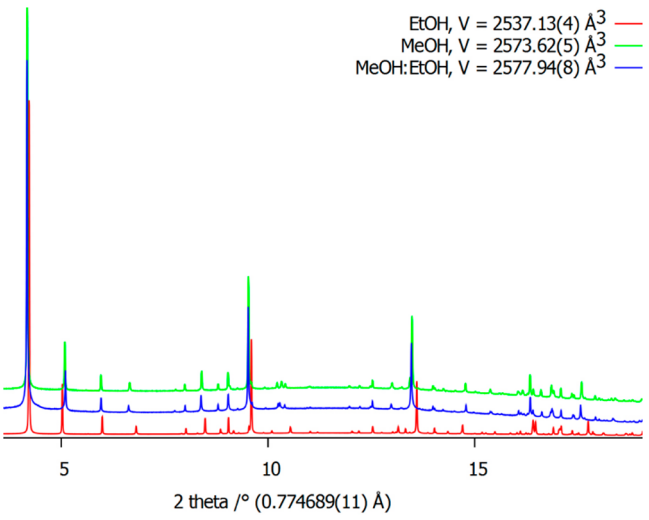

Figure 5. P-XRD pattern showing the preferable uptake of MeOH from an ME mixture by **Co-btca**.

the P-XRD pattern changed, indicating that in the absence of MeOH, EtOH can also be absorbed, although a complete structural characterization of this phase was not possible.

Unfortunately, single-crystal experiments on solvent soaked crystals resulted in too low data quality, suggesting that the solvent induced modification of the structure and the rapid loss of solvent alter the crystallinity of the sample.

DISCUSSION

In contrast with the initial classification,[26] **Co-btca** resulted a rather flexible MOF, not only because it shows an elastic behavior and a breathing effect similar to its Zn homologue[29] but also, more importantly, because the metal centers are able to selectively bind and release extra-framework molecules. This extraordinary functionality is favored by the open channel structure of the MOF architecture, suitable for hosting extra-framework nucleophiles which can directly interact with the metals under mild external stimuli. Although some organo-metallic compounds are already known to increase the metal coordinationunder pressure,[17−19] **Co-btca** is a remarkable and unprecedented example for MOFs, showing stepwise and reversible crystal to crystal reactions.

Nonoxidative nucleophilic additions are observed when **Co-btca** is filled with rather larger molecules of DMF as well as when DMF is replaced by the much smaller methanol.

When hydrostatically compressed with a nonpenetrating PTM, the extra-framework DMF molecules are capable of saturating part of the penta-coordinated Co atoms of the framework. Despite the availability of sufficient amount of DMF in the channels, a complete saturation is not favorable even at higher pressure. As a matter of fact, the unreacted DMF molecules assume an orientation which is unfavorable to coordinate the available Co ions, maximizing instead the packing density inside the channels.

Surprisingly, a similar host−guest reactivity is observed at moderate LT. A volumetric thermal contraction of only ca. 0.5% and the reduced thermal motion are in fact sufficient to cause the addition reaction with DMF, leading to a polymorph of partially saturated **Co-btca** and a more contracted volume (3%). The final products of the P- or T-induced coordination reaction show different conformation of the adduct and different orientation of the unreacted guests in the channel. Therefore, albeit similar, the HP and LT phases are not identical and should be considered as two (conformational) polymorphs.

Additional information can be gained by comparing the HP and LT behavior as a function of the eulerian strain[30] (Figure 6): besides the fact that with HP experiments a much wider strain range can be explored, it is worth noting that, even at comparable strains, the lattice deformations do not coincide. This is especially evident for the crystallographic *c* axis.

From multitemperature SC-XRD experiments (see SI), the latent molar volume of transition is ca. 7 $cm^3\ mol^{-1}$. Assuming that the unsaturated and partially saturated phases maintain a constant ΔU, we can calculate a pressure increase of ca. 0.6 GPa necessary to stabilize the denser phase with partial saturation of Co. As a matter of fact, the pressure-induced transition is observed at 0.4(2)GPa. Reversely, the $P\Delta V$ computed from the multipressure experiments enables estimating a ΔH of ca. 5.6 kJ mol^{-1}, close to the heat exchange (ca. 4 kJ mol^{-1}) measured with differential scanning calorimetry at ambient P. These results are fully compatible with very similar dissociation energies for the OH···DMF H-bond and the Co···DMF coordination. A reasonable estimation for the former is 15 kJ mol^{-1}.[31,32] Therefore, the Co···DMF coordination is also rather weak, in keeping with the observed Co···O distance, which is quite longer (2.275(3) Å at 198 K)

DOI: 10.1021/jacs.5b09231
J. Am. Chem. Soc. 2015, 137, 13072−13078

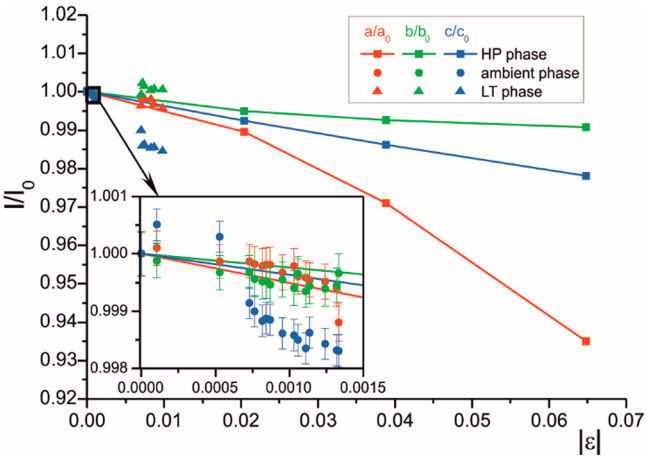

Figure 6. Relative compression as a function of the absolute eulerian strain for the lattice parameters of **Co-btca**·2 DMF·*n* H_2O from SC-XRD experiments.

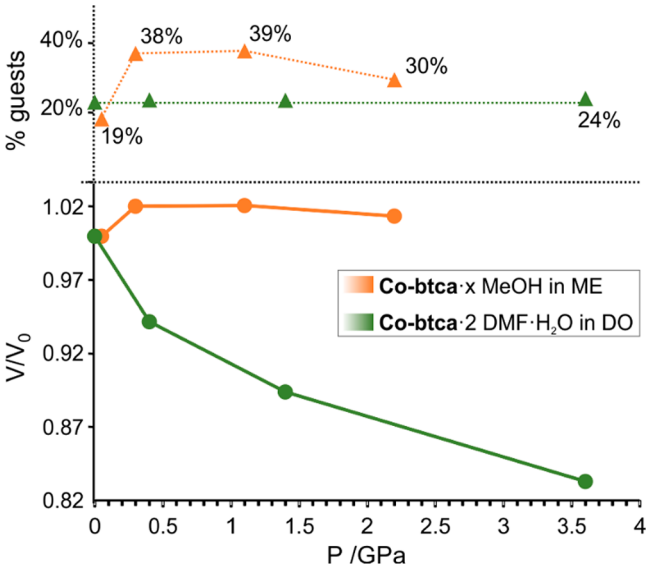

Figure 7. Comparison of the guest concentration (in weight percent) and relative unit-cell volume as a function of P for **Co-btca** in a penetrating (ME) and nonpenetrating (DO) PTM.

than for other DMF in octahedral Co complexes (1.940−2.267 Å).[33,34]

Co-btca selectively exchanges solvent molecules at ambient conditions, replacing DMF without modifying the structure of the framework and the lattice type. The more favorable uptake of MeOH from aME mixture is easily justified by the smaller size of the molecules, hence the easier access into the channels.

Once DMF is replaced, the reactivity of **Co-btca** filled with MeOH is even more intriguing, because a two-step nucleophilic addition occurs. The initial reaction mimics the behavior of the MOF filled with DMF, involving only half of the Co centers, preserving the crystallographic order, but reducing the crystal symmetry. The saturation of the remaining penta-coordinated Co requires a higher activation energy (i.e., higher pressure), and it eventually restores the monoclinic symmetry. It is likely that the second coordination reaction is possible for MeOH molecules, because they are less sterically hindered than DMF and are hosted in the channels in larger amount.

Penetrating PTMs were often found to promote P-induced uptake of additional guests, resulting in an initial increase of the crystal volume.[6,10,13] The completeness and the quality of the HP SC-XRD data sets are not sufficient to determine the exact content and positions of the highly disordered noncoordinated guests in the channels. Therefore, the P-induced MeOH uptake must be estimated indirectly, for example, using the SQUEEZE procedure implemented in the program PLATON.[28] The accuracy of this method is limited by the quality and the completeness of the diffraction data. Nevertheless, it enables comparing the guest content of a given sample at different pressures, given that the systematic errors in the diffraction measurements are similar in multipressure experiments. Moreover, SQUEEZE provides a fairly reliable and consistent estimation of the guest amount for **Co-btca**·2 DMF·H_2O (where the guest content is actually constant), despite the unavoidable incompleteness of HP-SC-XRD data. For **Co-btca**·*x* MeOH, the amount of guests estimated by SQUEEZE increases up to 1 GPa in analogy with the unit-cell volume increase (Figure 7). Above 1 GPa, the crystal shrinking overwhelms the channel filling, and the number of guest molecules starts decreasing.

The fact that an alternative intermediate phase was found in the range 0.6−0.9 GPa for some samples could depend on the initial amount of guests in the channels, which is poorly controllable during the MOF preparation or treatment. Although the different coordination and saturation of the metal centers implies different crystal symmetry during the compression, the flexibility of the framework and its sorption−desorption properties seem unaltered. In fact, the sample volume and the channel opening angles of all samples (SC or powders) increase smoothly and continuously up to ca. 1 GPa and afterward decrease slowly (see Figure 4).

The solvent exchange capacity significantly affects the mechanical response of the framework: the MeOH-superfilled **Co-btca** is significantly more rigid and less compressible than the as-prepared **Co-btca**·2 DMF·H_2O compressed in a nonpenetrating medium. In fact, the latter cannot absorb PTM molecules that would induce higher stability, and, in addition, it features some residual voids in the channels even at higher pressure, as witnessed by the persistence of orientational disorder of the noncoordinated DMF guests.

CONCLUSIONS

We have reported an unprecedented example of pressure-induced chemisorption in a flexible MOF, obtained through partial or full saturation of penta-coordinated metal centers. The nonoxidative nucleophilic addition occurs when pressure or temperature are varied. While P-induced conversion of nonbonding contacts to a metal into genuine coordinative bonds has been already reported, **Co-btca** MOF shows the remarkable ability to react with extra-framework ligands that are initially not interacting at all with the metal. The guest molecules are first captured in the **Co-btca** framework with the H-bonds hooks and afterward attached to the metal centers.

Such discovery can set the basis for the research of new promising materials with similar flexibility of the framework, in which easy and reversible coordinative reactivity can be exploited even for catalytic purposes.

Moreover, **Co-btca** proved to be a selectively absorbing material, a property that can be tuned by further functionalizing the channel surface. This could anticipate several applications, including molecular recognition or storage. For this reason we

DOI: 10.1021/jacs.5b09231
J. Am. Chem. Soc. 2015, 137, 13072−13078

are currently investigating isoreticular MOFs based on the same linkers but different metal ions.

METHODS

Synthesis. Single crystals of **Co-btca** were obtained combining cobalt(II) nitrate with H_2btca in a DMF/H2O mixture in solvothermal conditions. The product was preliminarly characterized by SC-XRD and thermal analyses.

Variable-Temperature SC-XRD. All measurements were carried out with an Oxford Diffraction SuperNova area-detector diffractometer using mirror optics monochromated Mo Kα radiation (λ = 0.71073 Å). The temperature was controlled with a Cryostream 700 by Oxford Cryosystems.

HP SC-XRD. Crystals of **Co-btca** were loaded in a Merrill-Bassett diamond anvil cell, equipped with 0.5 mm diamonds and pre-indented steel gaskets. DO or ME were used as PTM, and pressure was calibrated with the ruby fluorescence method.[35] All measurements were carried out with an Oxford Diffraction SuperNova area-detector diffractometer using mirror optics monochromated Mo Kα radiation (λ = 0.71073 Å).

Ambient Pressure P-XRD. Single crystals of **Co-btca** were ground, treated with different solvents or solvent mixtures, and filled into glass capillaries. Diffraction measurements were performed at the X04SA Materials Science Beamline at the Swiss Light Source, Paul Scherrer Institut, Villigen, Switzerland.[36]

HP P-XRD. Ground **Co-btca** was loaded in a membrane-driven DAC, equipped with 0.5 mm diamond anvils and pre-indented steel gaskets. ME was used as PTM, and the pressure was calibrated with the equation of state of quartz added as internal standard.[37] Diffraction measurements were performed at the X04SA Material Science Beamline at the Swiss Light Source, Paul Scherrer Institut, Villigen, Switzerland.[36]

ASSOCIATED CONTENT

Supporting Information

The Supporting Information is available free of charge on the ACS Publications website at DOI: 10.1021/jacs.5b09231.

Detailed experimental procedures (PDF)
Crystallographic information files(ZIP)
(AVI)

AUTHOR INFORMATION

Corresponding Authors

*piero.macchi@dcb.unibe.ch
*arianna.lanza@dcb.unibe.ch

Present Address

§Max-Planck Institute for Solid State Research, Heisenbergstr. 1, 70569 Stuttgart, Germany.

Notes

The authors declare no competing financial interest.

ACKNOWLEDGMENTS

We thank the Swiss National Science Foundation for financial support (project no. 144534). We thank Mrs. Beatrice Frey for performing the thermal analyses.

REFERENCES

(1) Hosseini, M. W. *New J. Chem.* **2010**, *34*, 2337.
(2) Kaskel, S.; Fischer, R. A. *J. Mater. Chem.* **2012**, *22*, 10093.
(3) Zhou, H.-C.; Kitagawa, S. *Chem. Soc. Rev.* **2014**, *43*, 5415.
(4) Long, J. R.; Yaghi, O. M. *Chem. Soc. Rev.* **2009**, *38*, 1213.
(5) Férey, G.; Serre, C. *Chem. Soc. Rev.* **2009**, *38* (5), 1380.
(6) Chapman, K. W.; Halder, G. J.; Chupas, P. J. *J. Am. Chem. Soc.* **2008**, *130*, 10524.
(7) Chapman, K. W.; Halder, G. J.; Chupas, P. J. *J. Am. Chem. Soc.* **2009**, *131*, 17546.
(8) Moggach, S. A.; Bennett, T. D.; Cheetham, A. K. *Angew. Chem., Int. Ed.* **2009**, *48* (38), 7087.
(9) Bennett, T. D.; Simoncic, P.; Moggach, S. A.; Gozzo, F.; Macchi, P.; Keen, D. a; Tan, J.-C.; Cheetham, A. K. *Chem. Commun.* **2011**, *47* (28), 7983.
(10) Graham, A. J.; Allan, D. R.; Muszkiewicz, A.; Morrison, C. A.; Moggach, S. A. *Angew. Chem., Int. Ed.* **2011**, *50* (47), 11138.
(11) Serra-Crespo, P.; Stavitski, E.; Kapteijn, F.; Gascon, J. *RSC Adv.* **2012**, *2* (12), 5051.
(12) Gagnon, K. J.; Beavers, C. M.; Clear, A. *J. Am. Chem. Soc.* **2013**, *135*, 1252.
(13) Graham, A. J.; Banu, A.; Du, T.; Greenaway, A.; Mckellar, S. C.; Mowat, J. P. S.; Ward, K.; Wright, P. A.; Moggach, S. A. *J. Am. Chem. Soc.* **2014**, *136*, 8606.
(14) Cai, W.; Gładysiak, A.; Anioła, M.; Smith, V. J.; Barbour, L. J.; Katrusiak, A. *J. Am. Chem. Soc.* **2015**, *137*, 9296.
(15) Spencer, E. C.; Kiran, M. S. R. N.; Li, W.; Ramamurty, U.; Ross, N. L.; Cheetham, A. K. *Angew. Chem., Int. Ed.* **2014**, *53* (22), 5583.
(16) Tan, J. C.; Cheetham, A. K. *Chem. Soc. Rev.* **2011**, *40* (2), 1059.
(17) Allan, D. R.; Blake, A. J.; Huang, D.; Prior, T. J.; Schröder, M. *Chem. Commun. (Cambridge, U. K.)* **2006**, *2* (39), 4081.
(18) Moggach, S. A.; Galloway, K. W.; Lennie, A. R.; Parois, P.; Rowantree, N.; Brechin, E. K.; Warren, J. E.; Murrie, M.; Parsons, S. *CrystEngComm* **2009**, *11* (12), 2601.
(19) Gould, J. a; Rosseinsky, M. J.; Moggach, S. a. *Dalton Trans.* **2012**, *41* (18), 5464.
(20) Lee, J. Y.; Lee, S. Y.; Sim, W.; Park, K.-M.; Kim, J.; Lee, S. S. *J. Am. Chem. Soc.* **2008**, *130* (22), 6902.
(21) Allan, P. K.; Xiao, B.; Teat, S. J.; Knight, J. W.; Morris, R. E. *J. Am. Chem. Soc.* **2010**, *132* (10), 3605.
(22) Avendano, C.; Zhang, Z.; Ota, A.; Zhao, H.; Dunbar, K. R. *Angew. Chem., Int. Ed.* **2011**, *50* (29), 6543.
(23) Zhao, N.; Sun, F.; He, H.; Jia, J.; Zhu, G. *Cryst. Growth Des.* **2014**, *14* (4), 1738.
(24) Coudert, F.-X. *Chem. Mater.* **2015**, *27* (6), 1905.
(25) Addison, A. W.; Rao, T. N.; Reedijk, J.; van Rijn, J.; Verschoor, G. C. *J. Chem. Soc., Dalton Trans.* **1984**, *7*, 1349.
(26) Zhang, X.-M.; Hao, Z.-M.; Zhang, W.-X.; Chen, X.-M. *Angew. Chem.* **2007**, *119* (19), 3526.
(27) Horike, S.; Shimomura, S.; Kitagawa, S. *Nat. Chem.* **2009**, *1* (9), 695.
(28) Spek, A. L. *Acta Crystallogr., Sect. C: Struct. Chem.* **2015**, *71* (1), 9.
(29) Xiao, J.; Wu, Y.; Li, M.; Liu, B. Y.; Huang, X. C.; Li, D. *Chem. - Eur. J.* **2013**, *19* (6), 1891.
(30) Birch, F. *Phys. Rev.* **1947**, *71* (11), 809.
(31) Feng, W.; Jia, G. *Phys. A* **2014**, *404*, 315.
(32) Koné, M.; Illien, B.; Laurence, C.; Graton, J. *J. Phys. Chem. A* **2011**, *115* (47), 13975.
(33) Allen, F. H. *Acta Crystallogr., Sect. B: Struct. Sci.* **2002**, *58* (3), 380.
(34) Bruno, I. J.; Cole, J. C.; Edgington, P. R.; Kessler, M.; Macrae, C. F.; McCabe, P.; Pearson, J.; Taylor, R. *Acta Crystallogr., Sect. B: Struct. Sci.* **2002**, *58* (3), 389.
(35) Syassen, K. *High Pressure Res.* **2008**, *28* (2), 75.
(36) Willmott, P. R.; Meister, D.; Leake, S. J.; Lange, M.; Bergamaschi, A.; Böge, M.; Calvi, M.; Cancellieri, C.; Casati, N.; Cervellino, A.; Chen, Q.; David, C.; Flechsig, U.; Gozzo, F.; Henrich, B.; Jäggi-Spielmann, S.; Jakob, B.; Kalichava, I.; Karvinen, P.; Krempasky, J.; Lüdeke, A.; Lüscher, R.; Maag, S.; Quitmann, C.; Reinle-Schmitt, M. L.; Schmidt, T.; Schmitt, B.; Streun, A.; Vartiainen, I.; Vitins, M.; Wang, X.; Wullschleger, R. *J. Synchrotron Radiat.* **2013**, *20*, 667.
(37) Angel, R. J.; Allan, D. R.; Miletich, R.; Finger, L. W. *J. Appl. Crystallogr.* **1997**, *30* (4), 461.

DOI: 10.1021/jacs.5b09231
J. Am. Chem. Soc. 2015, 137, 13072−13078